ISSN : 0974 - 7486 Volume 14 Issue 9

Materials Science

An Indian Journal

Full Paper

MSAIJ, 14(9), 2016 [337-346]

Heating and phyiso-mechanical characteristics of porous spinel developed by starch

Kumar Saurav*, Manas Ranjan Majhi, Vinay Kumar Singh
Department of Ceramic Engineering, Indian Institute of Technology (bhu), (INDIA)
E-mail: ksaurav.cool@gmail.com

ABSTRACT

The paper examines thermal properties of materials. The transient pulse method was used for specific heat, thermal diffusivity and thermal conductivity determination. Porous MgO was synthesis by heating pellets at 1100 °C for 1h. The resultant porous MgO was then immersed in an 10mol/L aluminium nitrate solution, dried, and reheated at 1300 ºC for 2h to convert it to spinel. The evaluation was performed with the help of mathematical apparatus used for study of fractal structures properties. The method results from generalized relations that were designed for study of physical properties of fractal structures. As it is shown these relations are in a good agreement with the equations used for the description of time responses of temperature for the pulse input of supplied heat.

KEYWORDS

Ceramics;
Thermogravimetric analysis (TGA);
Chemical synthesis;
Mechanical properties;
Microstructure.

INTRODUCTION

Among the suitable materials for energy saving purpose, porous ceramics are outstanding because they combine intrinsic ceramic properties, such as chemical inertness and refractoriness, with low thermal conductivity. Besides saving energy, the diminished heat loss to the environment also improves working conditions minimizing the employees' stress as a result of their exposure to high temperatures. Porous ceramic products cover wide range of advanced ceramic materials, which can be oxides ceramics: alumina, zirconia, or non-oxides ceramics:carbides, borides, nitrides, silicides. The properties of porous ceramic product depend on three main factors: the properties of the ceramic material of which the product is made; the topology (connectivity) and shape of the pores; and the relative density of the product. Novel pore-forming agents as well as other starting materials were produced in situ via a solution combustion process and were used to fabricate porous $MgAl_2O_4$ ceramics[1-7]. Meanwhile, pore formers and otherstarting materials for porous ceramics used in the conventional methods were first prepared separately and then mixed.

Among the techniques used to produce these materials (such as the addition of foaming agents and organic compounds), the pore generation via phase transformation presents key aspects, such as easy processing and the absence of toxic volatiles In this study, this technique was applied to produce porous ceramics by decomposing an EX potato known as

starch soluble $(C_6H_{10}O_5)n$. Porous MgO ceramics prepared at different sintering temperatures is studied. A porous spinel body was fabricated from porous MgO using a Novel techniques. MgO with 68% porosity was fabricated by heating compact from platelets at 1300 C for 1h. The resultant porous MgO was then immersed in an 10mol/L aluminium nitrate solution, dried, and reheated at 1300 C for 2h to convert it to spinel. After five solution treatments The porosity, compressive strength, bulk density,permeability,thermal conductivity are calculated and finally spinel conversion ratio are studied.

EXPERIMENTAL

Fine magnesium oxide (Thomas baker,India,0.10 mm in diameter and 98% pure)was used as a sintering additive. Ex potato starch (.50 mm, lobachemie) and PVA were also added to the starting materials as a pore former. All powders used as pore-formers were previously dried at 100 °C for 24 h. After this step, their density and surface area were measured in Accu Pyc 1330 helium pycnometer and BET equipment (Micrometrics, USA), respectively. The surface area of porous MgO are found 100 m^2/g. Lightly Calcined (fine powder) magnesia and EX Potato Starch - $C_6H_{10}O_{5N}$ (loba chemie, mumbai) was mixed and then poly vinyl alcohol (fine powder) are mixed. The batches were comprised of Porous MgO (60;30;10-MgO;Starch;PVA) were attrition milled for 3 h and then dried at 100°C for 24 h. The powders were shaped in pellet (piece of small shot) form using hydraulic pressing machine (uniform pressing) with applied load of 15 tonn.. The samples were fired at temperatures 1100°C. The heating rate was maintained at 3°C/min and soaking period was 2 hour. The sintered sample was immersed into the aluminium nitrate solution for 1 h under vacuum, removed, and then dried at room temperature for 24h. The resultant sample was reheated at 1300 ºC for 2h in air. This solution immersion and reheating treatment was performed up to five times. After each solution treatments are characterized by XRD,SEM, DTA, TGA, Thermal Conductivity, Permeability, Thermal diffusivity. Similar to the decomposition of organic matter, this technique is based on generating pores through the volume reduction that follows the decarbonation reactions[8-13]. The examples of industrially important porous materials include catalysts, construction materials, ceramics, pharmaceutical products, pigments, sorbents, membranes, electrodes, sensors, active components in batteries and fuel cells, and oil and gas bearing strata and rocks. The volume fraction of porosity can be defined as the fraction of void space relative to the apparent total bulk volume of the sample. Porosity in materials originates from different processing and synthesis routes. Synthesis of porous crystalline materials, such as magnesia compound and metal organic frameworks, leads to highly regular intra crystalline pore networks in addition to inherent voids imparted by the presence of vacancies, grain boundaries, and inter particle spaces[13-16]. As a simplified measure, pore size (or width) is referred to the smallest dimension within a given pore shape, that is, the width between two opposite walls for a slit-shaped pore and the diameter for a cylindrical pore. Pore volume fractions as a function of the time T_{max} are reported in TABLE 1. The micrograph in Figure 1 reveals a homogeneous pore size of less than 2 μm and variation in pore shape and size. At least two different characteristic pore sizes can be identified. The mercury porosimetry measurements

TABLE 1 : Pore volume fraction of the maximum temperature used in following time cycle

Sample	T_{MAX} (hour)	APPARENT POROSITY(%)
POROUS MgO	0	68
POROUS MgO with first solution treatments	24	63
POROUS MgO with second solution treatments	48	57
POROUS MgO with third solution treatments	72	54
POROUS MgO with fourth solution treatments	120	52
POROUS MgO with fifth solution treatments	144	48

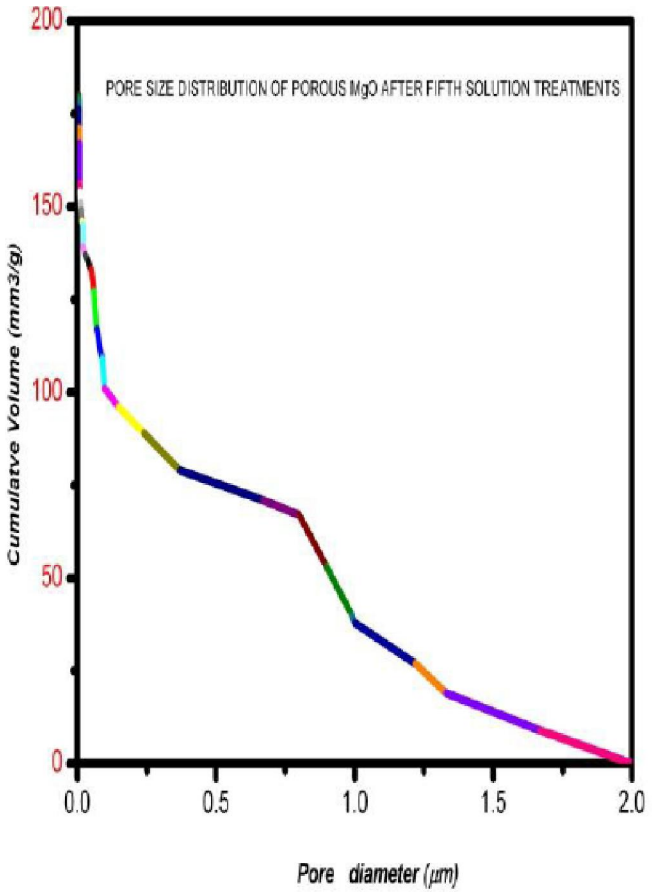

Figure 1 : Pore size distribution of porous MgO with fifth solution treatments sample contains (48%) porosity

confirm that the samples exhibit bimodal pore size distributions, constituted by mesopores with diameter less than 1 μm and by macropores with diameter above 1 μm.

DTA–TG analyses were carried out using a Netzsch STA409 equipment

RESULTS AND DISCUSSION

Spinel formation

The formation of the porous spinel from porous MgO and aluminium nitrate solution after fifth solution treatments was studied. Figure 2 a and Figure 2 b show DTA–TG analyses of the mixture, where the endothermic bands observed at 281æ%C and 345°C were attributed to dehydration and nitrate removal and removal of bound waters, respectively. At 1200 °C a small exothermic effect was detected associated with nucleation and formation of spinel by reaction between alumina and magnesia. This fact was confirmed by SEM and XRD diffraction studies. No distinct weight loss is observed at temperature higher than 800 °C because of the mass formation of spinel[17].

Figure 3. shows diffraction pattern of porous MgO with number of aluminium nitrate solution treat-

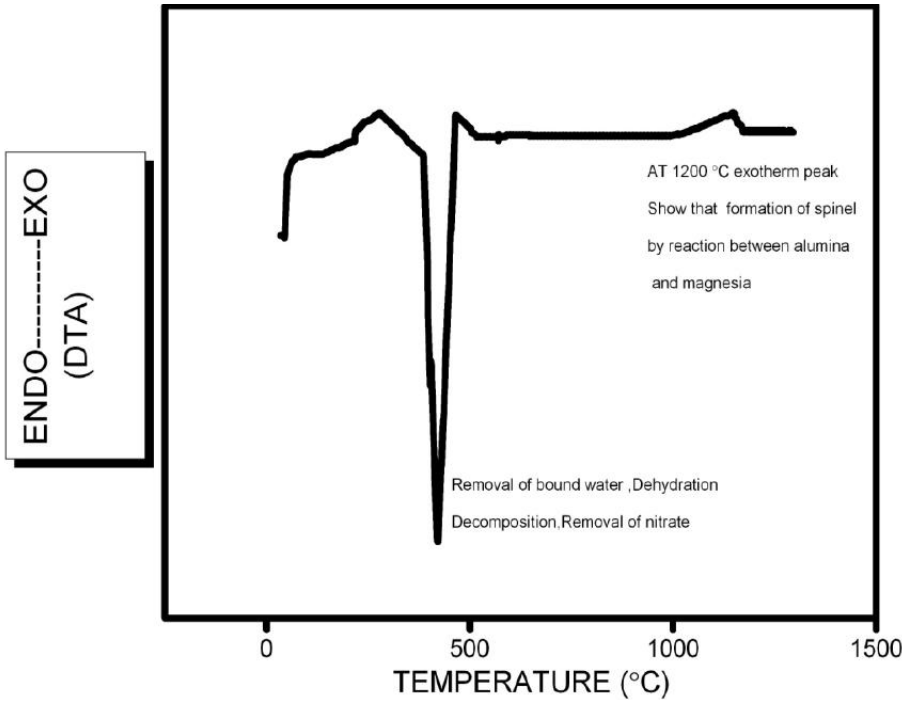

Figure 2a : A DTA of porous MgO after fifth solution treatments

Full Paper

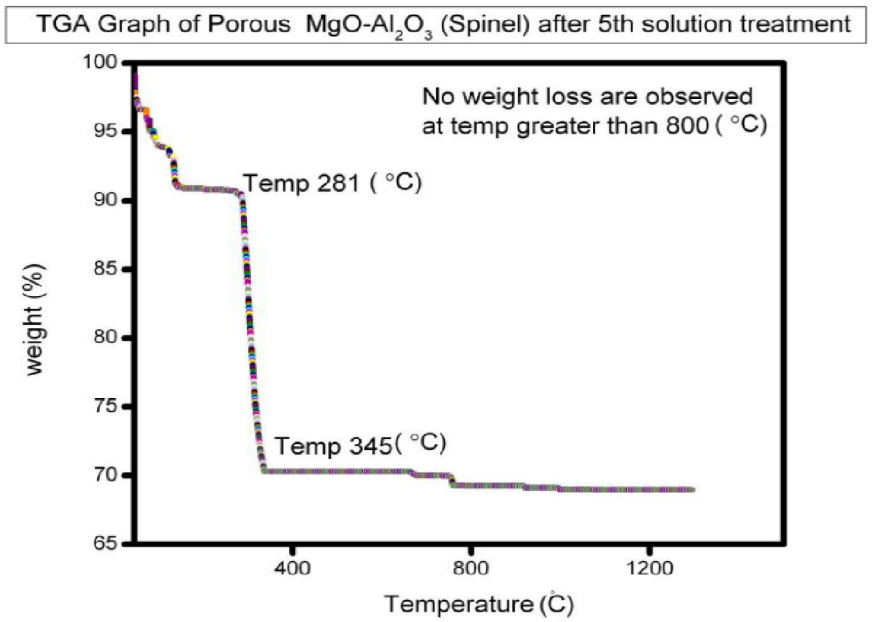

Figure 2b : TGA of Porous MgO after fifth solution treatments

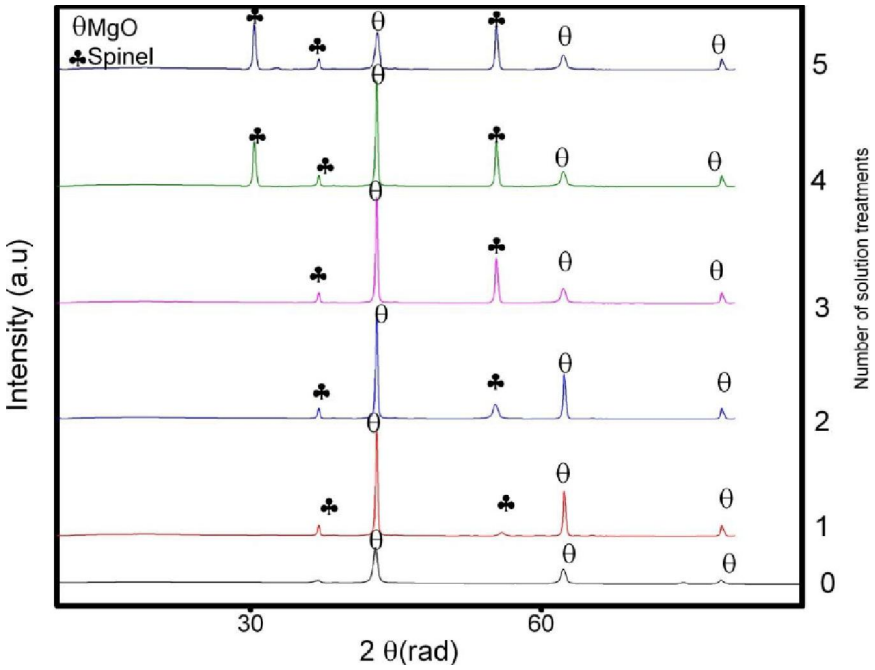

Figure 3 : XRD of Porous MgO with solution treatments

ments. Initially after first solution treatment a small peaks of spinel are detected,which indicated that the MgO reacts with alumina and forms spinel. As can be seen, no alumina was detected in any sample, which indicates that the initially precipitated alumina completely reacted with MgO to form Spinel during processing. After five solution treaments huge amount of spinel are formed. The ratio of spinel conversion are calculated by weight gain formula according to the chemical reaction. Actually more than 35% Spinel are formed after the fifth solution treatments.

Figure 4a Shows an SEM micrograph of a porous MgO sample without any treatments. The surfaces of the platelets were rough, but the overall platelet shape remained. The spot develop on the surface indicates the starch evolution during increasing temperature. Figure 4 b Shows an SEM micrograph of a porous MgO sample with first solution treatments. The white surface suggests that the MgO

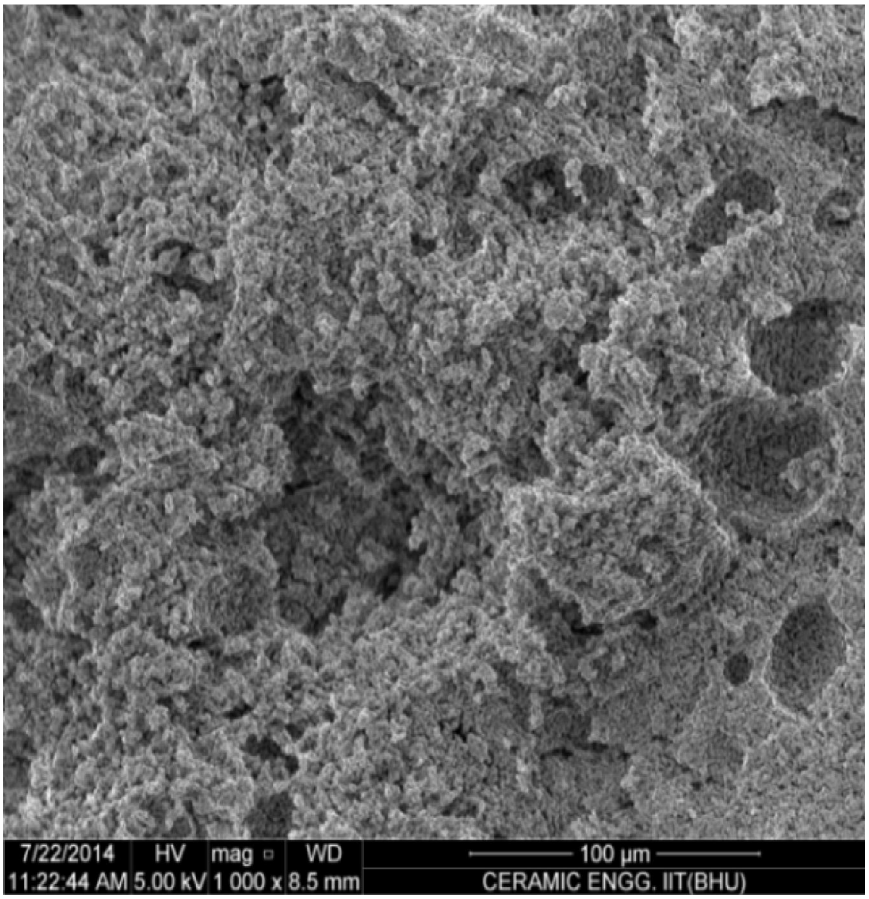

Figure 4a : SEM of Porous MgO with out solution treatments

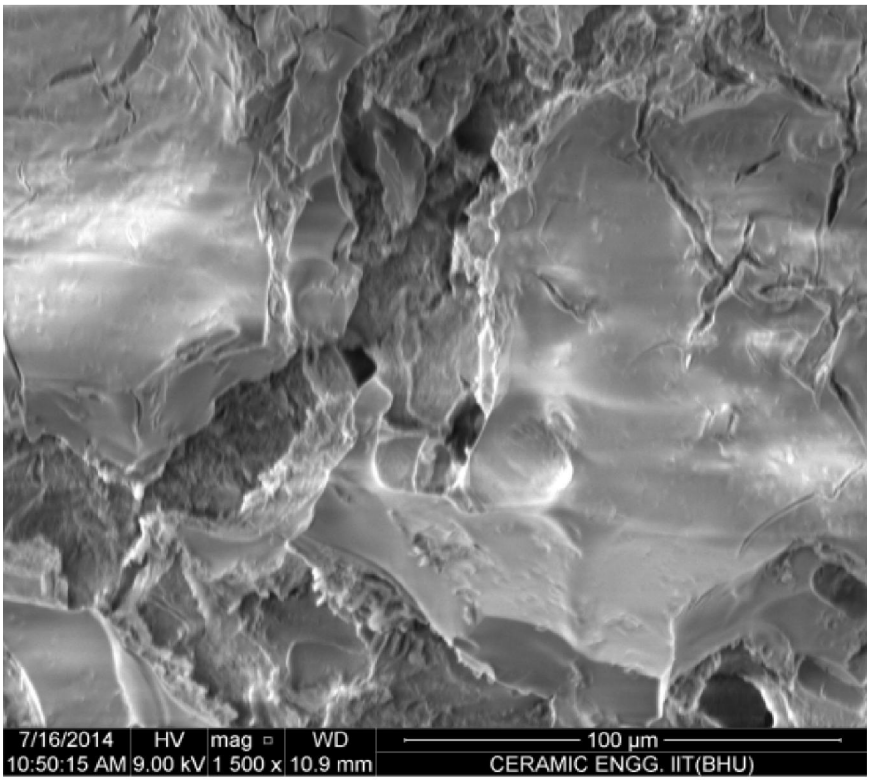

Figure 4b : SEM of Porous MgO with first solution treatments

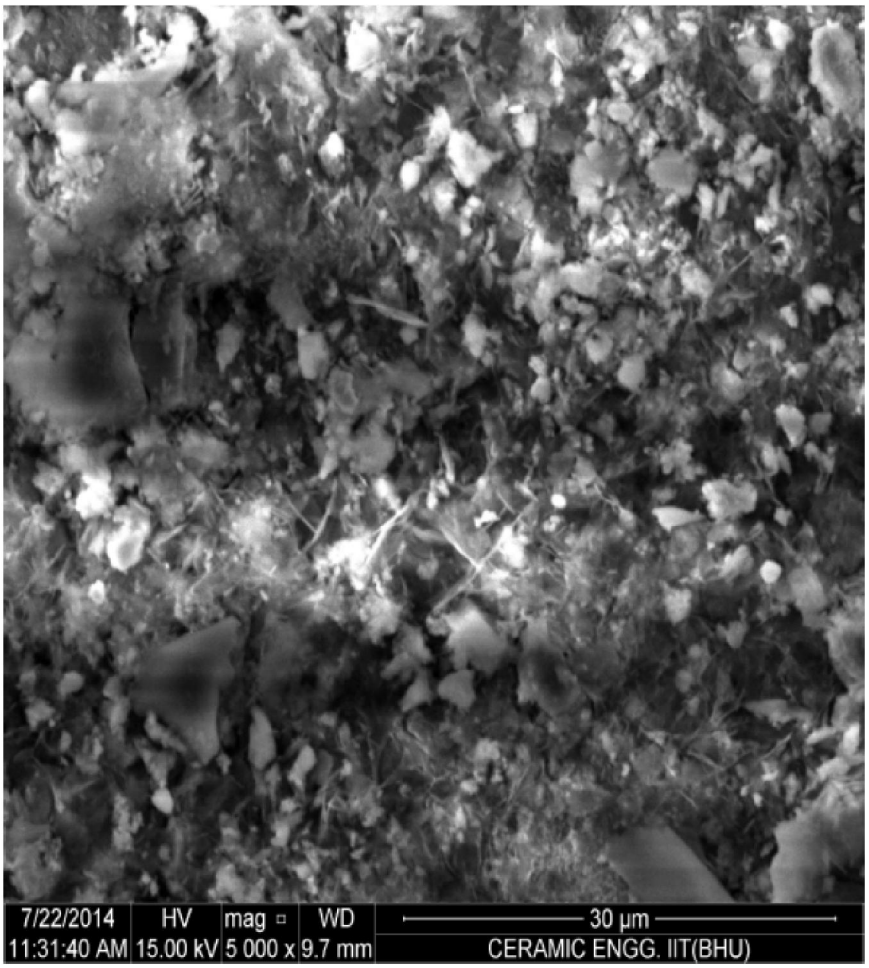

Figure 4c : SEM of Porous MgO with fifth solution treatments

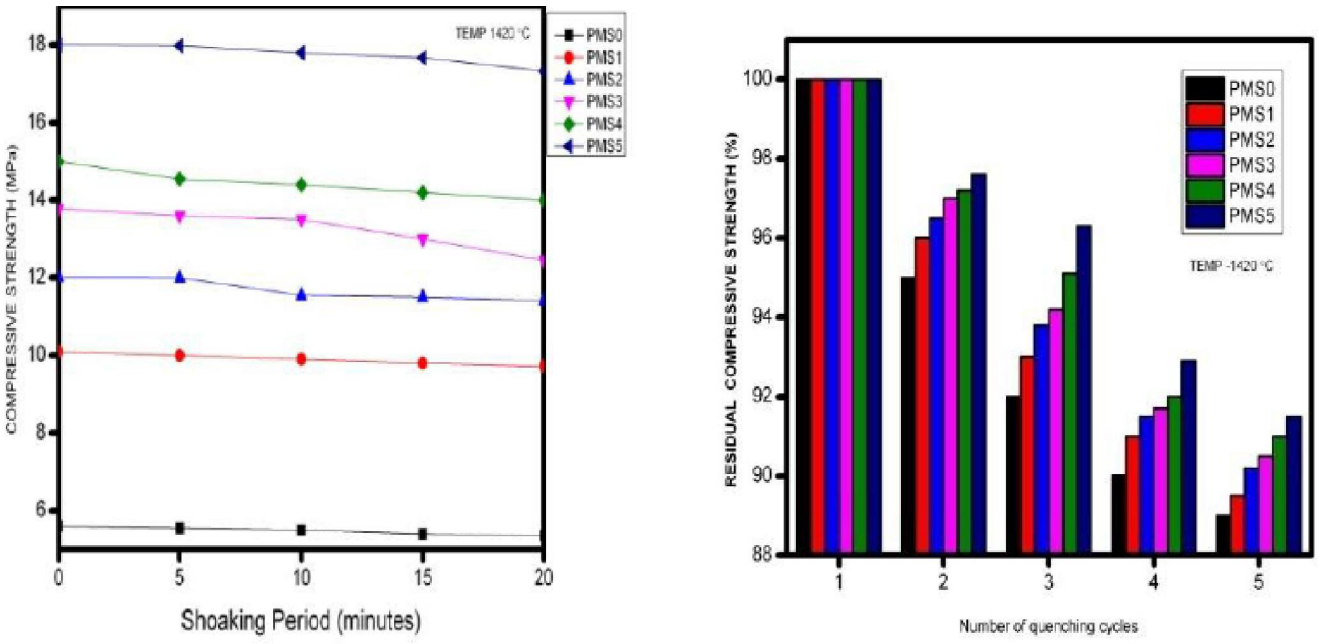

Figure 5 : Thermal shock of porous MgO vs number of solution treatments

platelets were partially covered with the precipi- tated spinel. Figure 4c Shows an SEM micrograph

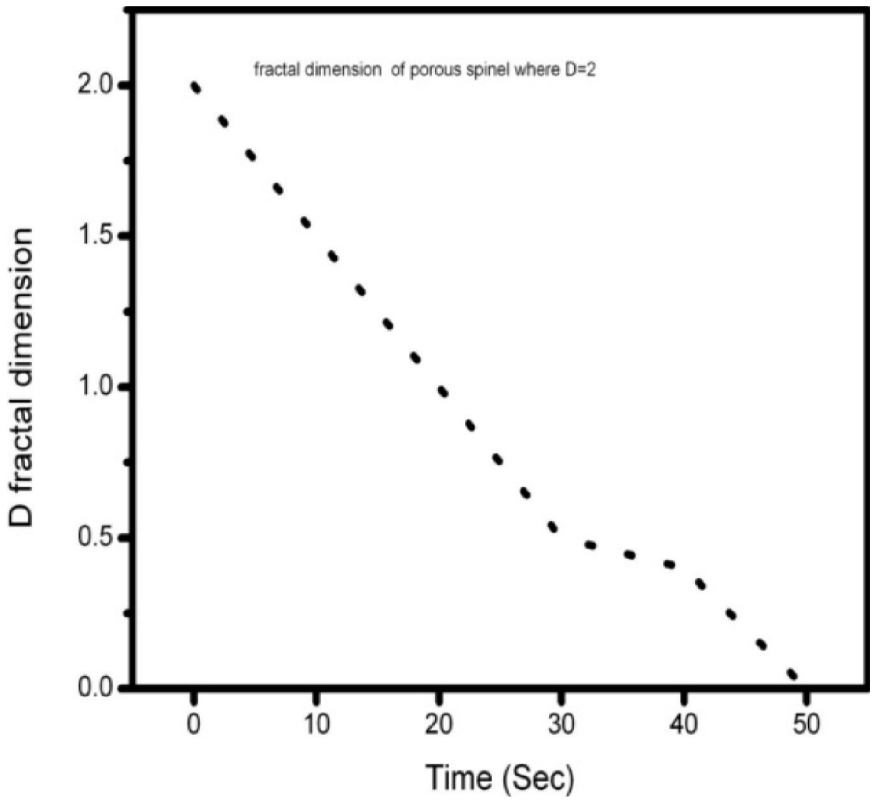

Figure 6a : Typical time responses of temperature for the Step wise of input power when D=2

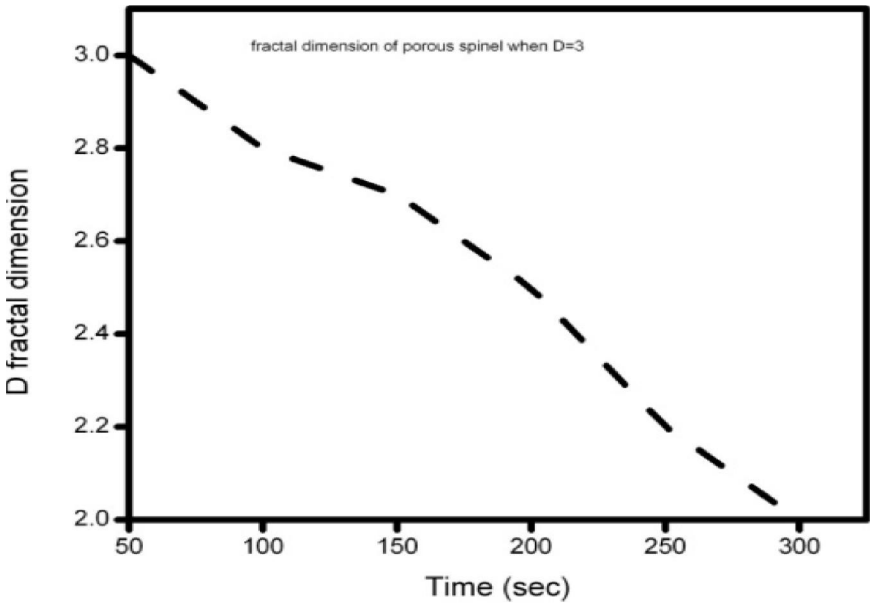

Figure 6b : Typical time responses of temperature for the step wise of input power when D=3.

of a porous MgO sample with fifth solution treatments,a large amount of white ball are developed which indicate huge amount of Spinel are formed. This suggests that the alumina Platelets were fully Covered with the Precipitated Spinel.

Thermal shock

An indentation-quench method for measuring thermal shock resistance of the ceramic was used. From Figure 5 parameters such as sample thickness, initial crack length, and water bath temperature were surveyed. It was found that one single sample could be used throughout a whole test series of different

Full Paper

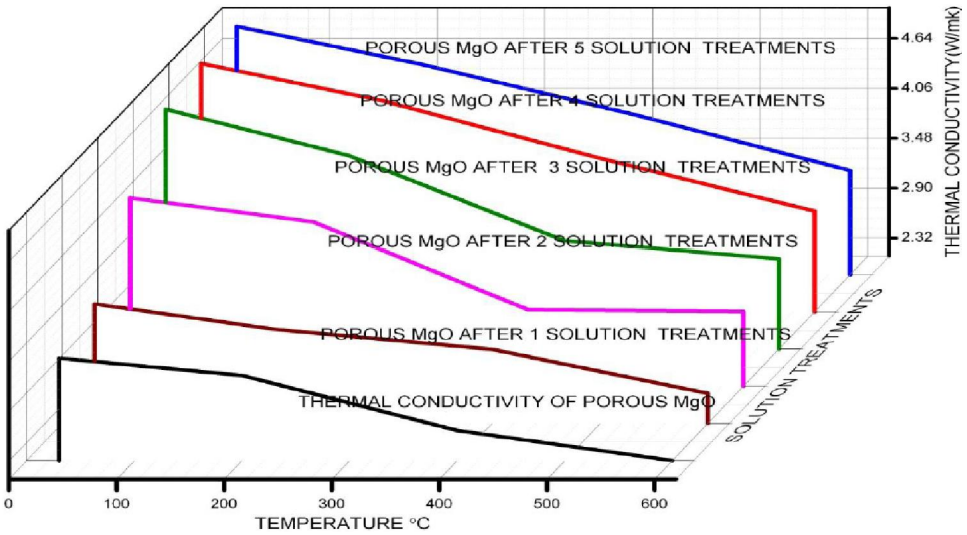

Figure 7 : Thermal conductivity of the porous MgO for each solution treatments

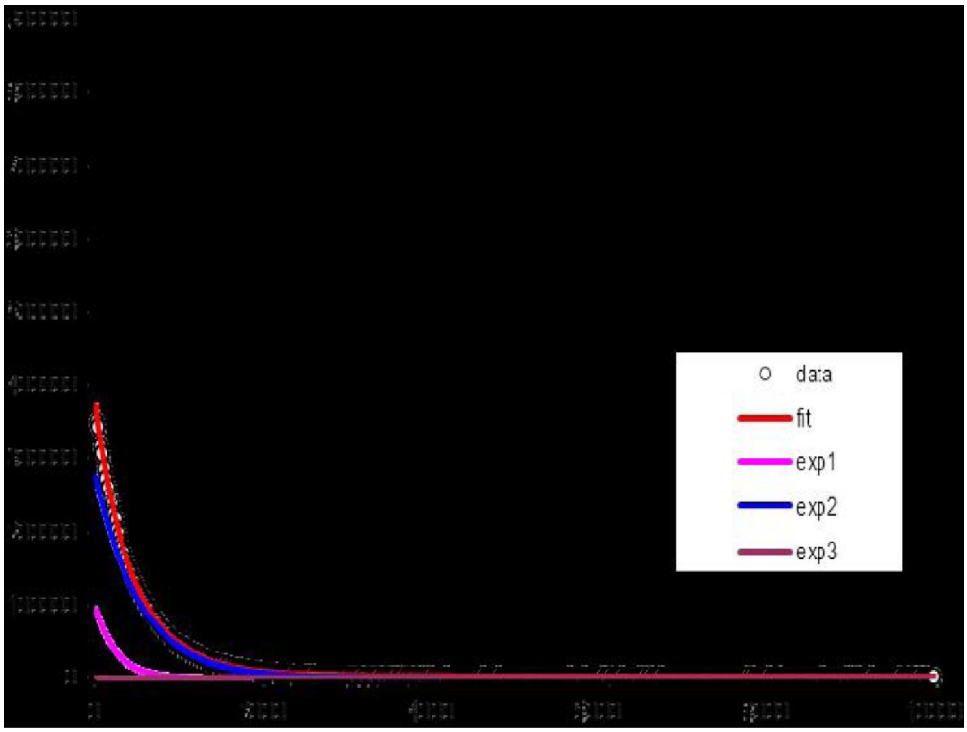

Figure 8 : Measured signal decays for porous spinel are associated with the rotating-frame spin-lattice relaxation time

quenching temperatures. The method can detect small differences in thermal shock resistance between materials, and was applicable to investigating thermal fatigue. The evaluation of thermal shock resistance of ceramics is crucial for components to be used at medium or high temperature or for tribological applications

Thermal behaviour

The transient pulse method was used for specific heat, thermal diffusivity and thermal conductivity determination. The evaluation was performed with the help of mathematical apparatus used for study of fractal structures properties Incorporation of porosity into a monolithic material decreases the effective thermal conductivity. The Figure 6a,6b represents the typical time responses of temperature for the step wise of input power. The coefficient f (fractal dimension D respectively) of the fractal heat[a]

source for every point of the experimental dependence (measured temperature depended on time) was calculated. The fractal heat source characterizes the distribution of the temperature in the specimen in specific time. From the Figure 6a and 6 b it is evident that for very short time there is the value of the fractal dimension $D \approx 2$ and therefore, the plane heat source is formed. The value of the fractal dimension decreases with increasing time value since the heat disperses into the space. From the time $\tau_1 \approx 16$ s (the intersection of tangents of the curves) the fractal dimension is getting settled to the value $D \approx 0{,}15$. The spatial distribution of the temperature in the sample does not change yet in this area. It is possible to determine the coefficient of the heat source $f_{a0} = 1$ and the diffusivity of the specimen from the extrapolated value of the fractal dimension to the time t = 0. Figure 7 shows that with increasing solution treatments,the thermal conductivity of the sample increased,finally reaching 4.8W/m1K1 after five solu- tion treatments. In these porous samples, the pore diameter was several micrometers due to the size of the platelets. Further more, the temperature remained below 600 ºC.

Water retention

The NMR measurements in this study aimed at determining the relative amounts of different water types in water-saturated clay samples The measurements were carried out with a high-field Chemagnetics CMX Infinity 270 MHz NMR spectrometer using a spin-locking CPMG technique. Briefly, From, Figure 8 that the measured signal decays are associated with the rotating-frame spin-lattice relaxation time, T1ρ. The use of the CPMG method to measure T1ρ is advantageous, since the whole decay signal can be obtained in one shot and a finer resolution of the deacay can be obtained for a given time. The measurement of T1ρ necessitates that all CPMG measurements are carried out with the same inter-pulse spacing τ in order to allow proper comparisons between results from different samples (Carlsson et al. 2012 and references therein). The software peak-o-mat (Kristukat 2008) was used to fit discrete exponentials to the decay curves obtained from the NMR measurements. The sample temperature was kept at 23 °C by gas flushing.

CONCLUSION

Porous ceramics for applications such as to reduce energy costs, high-temperature insulation can be produced by the decomposition of EX potato known as starch soluble $(C_6H_{10}O_5)n$. In this article, the results of thermal responses to the pulse of supplied heat evaluations are discussed. To interpret the outcomes, the simplified heat conductivity model is used. The coefficient f_a (fractal dimension D respectively) of the fractal heat source for every point of the experimental dependence (measured temperature depended on time) was calculated using the graph. NMR smeasurements were considered to contain contributions from several relaxation processes in the sample, and mathematical analyses of the exponential decays indicated the presence of several relaxation mechanisms. represents the typical time responses of temperature for the step wise of input power.

REFRENCES

[1] V.R.Salvini, M.D.M.Innocentini, V.C.Pandolfelli; Optimizing permeability, Mechanical strength of ceramic foams, American Ceramic Society Bulletin, **79(5)**, 49–63 **(2000)**.

[2] O.Zmeškal, M.Nežádal, M.Buchníček; Fractal–cantorian geometry, Hausdorff dimension and the fundamental laws of physics, Chaos, Solitons & Fractals, **17**, 113–119 **(2003)**.

[3] O.Lyckfeldt, J.M.F.Ferreira; Processing of porous ceramics by starch consolidation, Journal of the European Ceramic Society, **18(2)**, 131–140 **(1998)**.

[4] H.C.Park, Y.B.Lee, K.D.Oh, F.L.Riley; Grain growth in sintered MgAl2O4 spinel, Journal of Materials Science Letters, **16**, 1841–1844 **(1997)**.

[5] T.C.Farrar, Becker; Pulse and fourier transform NMR: Introduction to theory and methods, Academic Press, New York **(1971)**.

[6] R.Sarkar, S.K.Das, G.Banerjee; Effect of attrition milling on the densification of magnesium aluminate spinel, Ceramics International, **25**, 485–489 **(1999)**.

[7] Y.Suyama, A.Kato; Characterization and sintering of Mg–Al spinel prepared by spray-pyrosis technique, Ceramics International, **8**, 17–21 **(1982)**.

[8] A.R.Studart, U.T.Gonzenbach, E.Tervoot, L.J.Gauckler; Processing routes to macroporous ceramics: A review, Journal of the American Ceramic Society, **89(6)**, 1771–1789 **(2006)**.

[9] C.T.Wang, L.S.Lin, S.J.Yang; Preparation of MgAl2O4 spinel powders via freeze-drying of alkoxide precursors, Journal of the American Ceramic Society, **75**, 2240–2243 **(1992)**.

[10] J.Katanic Popovic, N.Miljevic, S.Zec; Spinel formation from coprecipitated gel, Ceramics International, **17**, 49–52 **(1991)**.

[11] T.Shiono, K.Shiono, K.Miyamoto, G.Pezzotti; Synthesis and characterization of MgAl2O4 spinel powder from a heterogeneous alkoxide solution containing fine MgO powder, Journal of the American Ceramic Society, **83**, 235–237 **(2000)**.

[12] K.C.Patil, M.S.Hegde, Rattan Tanu, S.T.Aruna; Chemistry of nanocrystalline oxide materials: combustion synthesis, Properties and Applications.Singapore, World Scientific Press, **(2008)**.

[13] U.T.Gonzenbach, A.R.Studart, E.Tervoot, J.L.Gauckler; Macroporous ceramics from particle-stabilized wet foams, Journal of the American Ceramic Society, **90(1)**, 16–22 **(2007)**.

[14] U.T.Gonzenback, A.R.Studart, D.Steinlin, E.Tervoot, J.L.Gauckler; Processing of particle-stabilized wet foams into porous ceramics, Journal of the American Ceramic Society, **90(11)**, 3407–3414 **(2007)**.

[15] W.Mista, J.Wrzyszcz; Rehydration of transition aluminas obtained by flash calcination of gibbsite, Thermochimica Acta, **331(1)**, 67–72 **(1999)**.

[16] Z.Deng, T.Fukasawa, M.Ando; High-surface-area alumina ceramics fabricated by the decomposition of Al(OH)3, Journal of the American Ceramic Society, **84(3)**, 485–491 **(2001)**.

[17] K.Saurav, M.Majhi, V.Singh; Preperation and characterization of high strength and high porosity porous spinel by decomposing an EX - POTATO known as starch soluble (C6H10O5)N using porous magnesia, Int.J.Porous Mater., **5(1)**, **(2015)**.